Supporting Information

Chemical State Modulation of Tungsten via High-Electronegativity Nonmetallic Elements for Enhanced Electrochemical Energy Storage

Zefeng Chen[abc], Huan Liu[abc], Xingwei Sun[abc], Qi Wang[abc], Weiyan Sun[abc*]

[a] *College of Chemical Engineering, Inner Mongolia University of Technology, 49 Aimin Street, Hohhot 010051, Inner Mongolia, P. R. China*

[b] *Inner Mongolia Key Laboratory of Green Chemical Engineering, 49 Aimin Street, Hohhot 010051, Inner Mongolia, P. R. China*

[c] *Key Laboratory of Industrial Catalysis at Universities of Inner Mongolia Autonomous Region, 49 Aimin Street, Hohhot 010051, Inner Mongolia, P. R. China*

1.1 Material Characterization

The morphologies and structures of the samples were characterized using scanning electron microscopy (SEM, Quattro S, Thermo Fisher Scientific, USA) and transmission electron microscopy (TEM, Talos F200X, Thermo Fisher Scientific, USA). Raman spectra were recorded (Raman, DXR3 Flex, Thermo Fisher Scientific, USA, laser wavelength: 532 nm, resolution: 5.5 cm^{-1}, number of scans: 2 consecutive scans) to analyze molecular vibrational modes. Crystallization characteristics were analyzed by X-ray diffraction (XRD, XRDynamic 500, Anton Paar, Austria) at a voltage of 40 kV and a current of 50 mA, with Cu Kα radiation (λ = 0.15406 nm). Surface chemical composition and valence states were determined through X-ray photoelectron spectroscopy (XPS, Esclab 250xi, Thermo Fisher Scientific, USA) using an Al Kα X-ray source (hv = 1486.6 eV), and the C 1s peak of adventitious carbon (binding energy = 284.8 eV) was used for calibration. Electrochemical measurements were performed on a CHI760E electrochemical workstation (Shanghai Chenhua, China).

SEM specimen preparation protocol: Specimens were trimmed to appropriate dimensions according to the sample stage size. Surfaces were gently cleaned with anhydrous ethanol-soaked lint-free wipes to remove adsorbed contaminants. Specimens were mounted centrally on conductive adhesive tape with even pressure application for optimal contact. Loose particles were removed by ultra-pure nitrogen gas blowing. Gold coating with approximate 5 nm thickness was applied using an ion sputtering coater. Coated samples were placed in a desiccator for 30 minutes to stabilize coatings and remove moisture. Sample stage assemblies were loaded into SEM vacuum chamber for observation.

TEM specimen preparation protocol: Carbon fiber-supported powder samples were trimmed to appropriate dimensions. The trimmed samples were placed in a centrifuge tube with 2 mL high-purity ethanol as dispersant. Samples in the centrifuge tube were ultrasonically treated (300 W) for 10 min to detach and disperse particles into mono-/small aggregates. 2 μL suspension aliquots were pipetted onto carbon-coated copper grids. The grids were air-dried in a laminar flow hood until complete solvent evaporation. The carbon fibres and dispersed powder particles have been stably adhered to the copper mesh surface, and the sample is ready for subsequent TEM observation.

XPS peak deconvolution analysis was conducted using Avantage 5.9931 software to resolve chemical states of target elements. The procedure included three steps: (1) Spectral preprocessing: The Shirley background subtraction method was applied to raw spectra; the C 1s peak calibrated at 284.8 eV served as reference for binding energy determination; (2) Fitting function selection: A Lorentzian-Gaussian mixed function (0.3 ratio) was selected; chemical states were identified based on elemental characteristics, with full width at half maximum (FWHM) constrained to avoid overfitting; (3) Fitting validation: Iterative parameter optimization (position, height, shape ratio) was performed until minimal residuals between fitted and experimental spectra were achieved.

1.2 Electrochemical Characterization

The prepared $W_{18}O_{49}$/OCC and WSe_2/OCC materials were cut into 1×1 cm^2 pieces to serve directly as working electrodes. A three-electrode system was employed for electrochemical testing: a platinum mesh

functioned as the counter electrode, an Ag/AgCl electrode as the reference electrode, and a 1 M H_2SO_4 aqueous solution as the electrolyte. The system was used to evaluate the materials' performance through cyclic voltammetry (CV), galvanostatic charge-discharge (GCD), and electrochemical impedance spectroscopy (EIS). The specific capacitance (C, F g^{-1}) was calculated according to the following equation:

$$C = \frac{I \times \Delta t}{m \times \Delta V} \tag{S1}$$

In this equation, C denotes specific capacitance; I corresponds to discharge current; Δt represents discharge duration; ΔV defines the potential window; and m indicates active substance mass.

The calculation method for Coulombic efficiency is as follows:

$$Coulombic\ efficiency\ (\%) = \frac{discharge\ time}{charge\ time} \times 100\% \tag{S2}$$

An ASC was constructed using the WSe_2/OCC electrode as the positive electrode and AC/OCC as the negative electrode. The mass of each electrode was calculated as follows:

$$\frac{m_+}{m_-} = \frac{C_- \times \Delta V_-}{C_+ \times \Delta V_+} \tag{S3}$$

Where m is the mass of the active material, ΔV represents the potential window of both electrodes, and C denotes the specific capacitance of each electrode. The calculated mass ratio of the positive to the negative electrode is 1.26.

The energy density (E) and power density (P) of the ASC are calculated as follows:

$$E = \frac{1}{7.2} \times C \times (\Delta V)^2 \tag{S4}$$

$$P = 3600 \times \frac{E}{\Delta t} \tag{S5}$$

The electrochemical reaction kinetics for the $W_{18}O_{49}$/OCC and WSe_2/OCC electrodes are calculated as follows:

$$i = av^b \tag{S6}$$

$$i = k_1 v + k_2 v^{0.5} \tag{S7}$$

In this equation, i denotes the measured current (A); a and b are constants; k_1 and k_2 correspond to the slope and intercept of the plots of i_t $v^{0.5}$ and $v^{0.5}$, respectively; and v is the scan rate (mV s^{-1}).

1.3 Material characterization and electrochemical tests

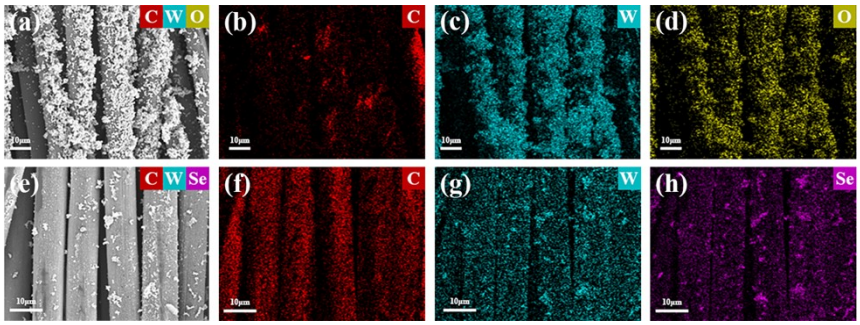

Fig. S1 EDS mapping images of (a-d) $W_{18}O_{49}$/OCC and (e-h) WSe_2/OCC.

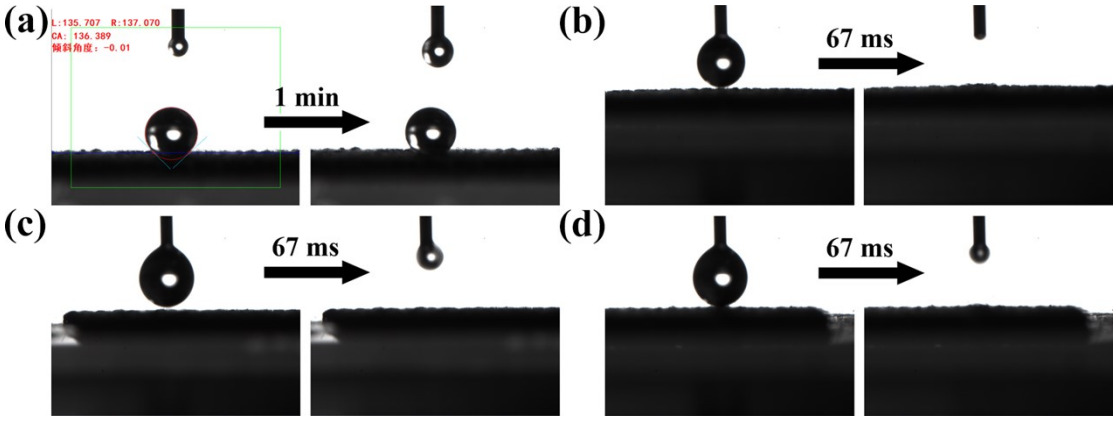

Fig. S2 Contact angle wettability measurements of (a) CC, (b) OCC, (c) $W_{18}O_{49}$/OCC and (d) WSe_2/OCC samples.

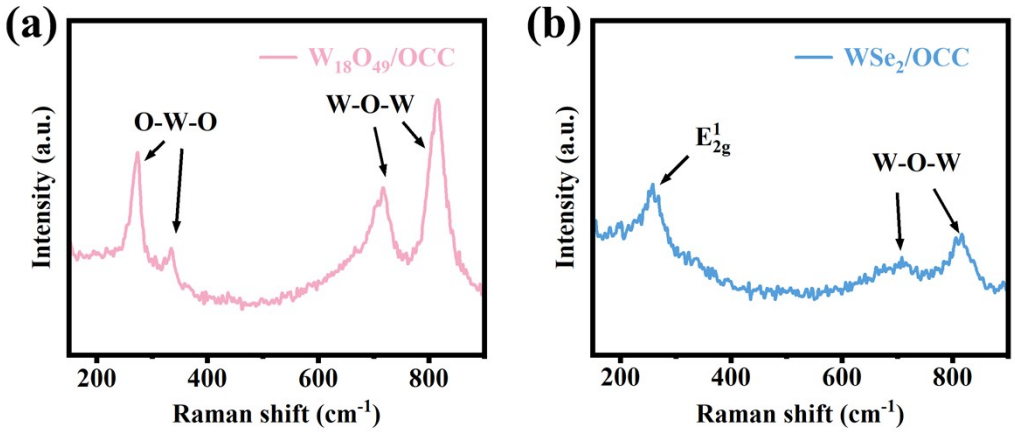

Fig. S3 Raman spectra of (a) $W_{18}O_{49}$/OCC and (b) WSe_2/OCC.

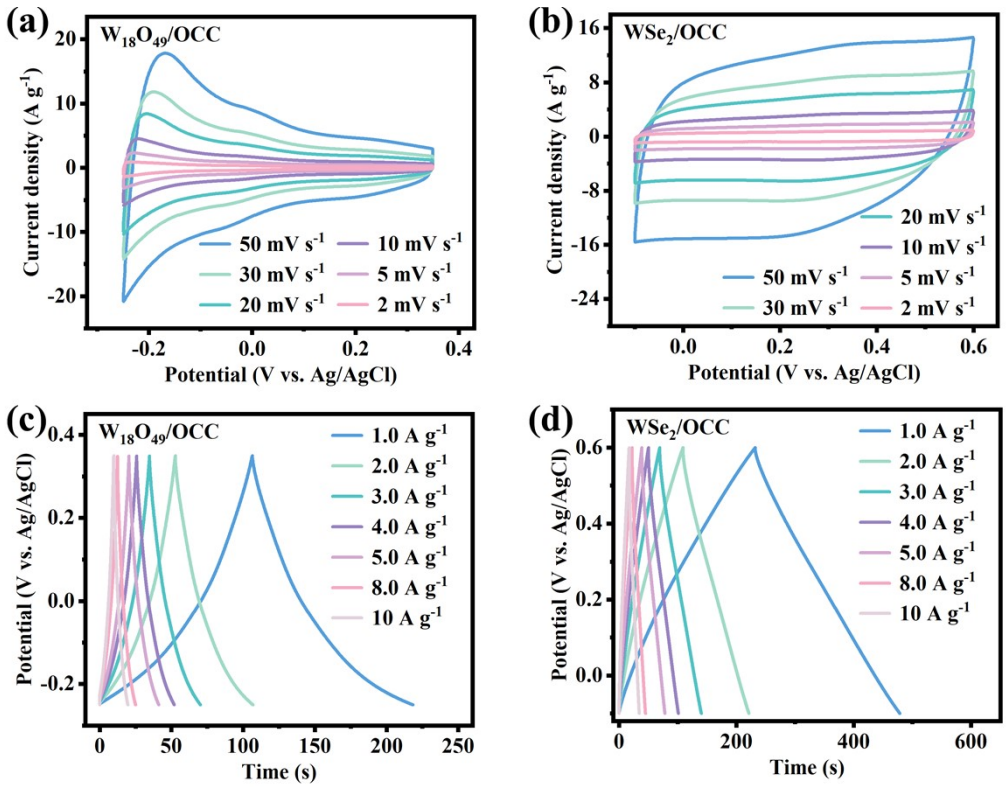

Fig. S4 The CV curves of (a) $W_{18}O_{49}$/OCC and (b) WSe_2/OCC at different sweep speeds. the GCDs of (c) $W_{18}O_{49}$/OCC and (d) WSe_2/OCC electrodes at different applied currents.

The asymmetric supercapacitor (ASC) was assembled using WSe_2/OCC as the positive electrode, AC/OCC as the negative electrode, 1 M H_2SO_4 as the electrolyte, and a glass fiber membrane as the separator. The device was configured in a button-type cell for electrochemical performance testing. The ASC delivers an energy density of 28.78 Wh kg^{-1} at a power density of 1.46 kW kg^{-1} [1-4].

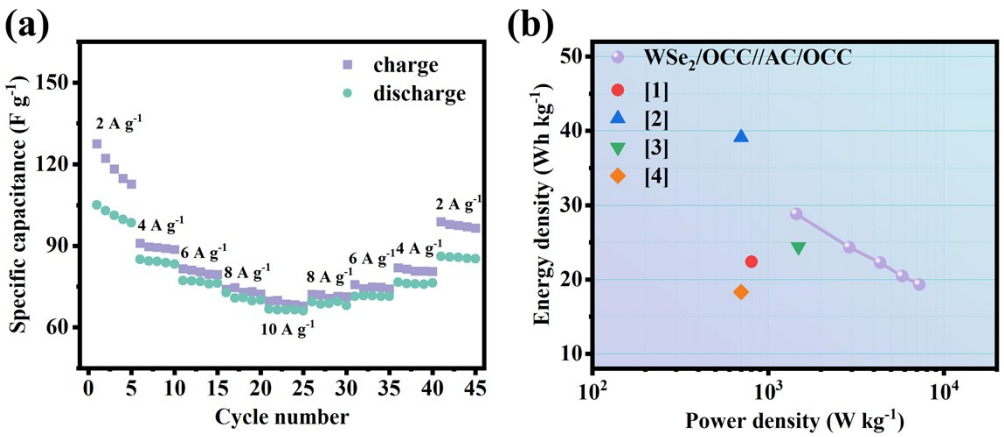

Fig. S5 (a) Rate capability plot of the WSe_2/OCC//AC/OCC button-type asymmetric supercapacitor (ASC) and (b) Ragone plot of the ASC

Table S1 W 4f spectral fitting paramaeters of undoped $W_{18}O_{49}$/OCC and WSe_2/OCC.

Material name	Valence state	Binding energy (eV)		Area		Area proportion (%)
		W $4f_{5/2}$	W $4f_{7/2}$	W $4f_{5/2}$	W $4f_{7/2}$	
$W_{18}O_{49}$/OCC	W^{6+}	37.78	35.66	40593.66	51441.63	91.40
	W^{5+}	36.37	34.25	3817.90	4838.16	8.60
WSe_2/OCC	W^{6+}	38.38	36.26	3206.21	4063.02	19.11
	W^{5+}	35.45	33.33	950.68	1204.74	5.66
	W^{4+}	34.43	32.31	12626.91	16001.24	75.23

References

1. J. Wu, G. Hu, J. Zhao, C. Zou, H. Xing, W. Shen and Z. Li, *Appl. Surf. Sci.*, 2024, **663**, 160136.
2. K. Pandey and H. K. Jeong, *J. Alloys Compd.*, 2024, **1008**, 176784.
3. H. Peng, R. Zhao, J. Liang, S. Wang, F. Wang, J. Zhou, G. Ma and Z. Lei, *ACS Appl. Mater. Interfaces*, 2018, **10**, 37125-37134.
4. Y. Li, W. Zhou, X. Duan, D. Li, J. Xu, Z. Huang and X. Hao, *J. Energy Storage*, 2024, **104**, 114560.